

See discussions, stats, and author profiles for this publication at: <https://www.researchgate.net/publication/231240070>

# Cyanonaphthalene Diimide Semiconductors for Air-Stable, Flexible, and Optically Transparent n-Channel Field-Effect Transistors

ARTICLE *in* CHEMISTRY OF MATERIALS · APRIL 2007

Impact Factor: 8.35 · DOI: 10.1021/cm0704579

---

CITATIONS

172

---

READS

60

4 AUTHORS, INCLUDING:



Antonio Facchetti

Northwestern University

381 PUBLICATIONS 22,186 CITATIONS

SEE PROFILE

# CHEMISTRY OF MATERIALS

VOLUME 19, NUMBER 11

MAY 29, 2007

© Copyright 2007 by the American Chemical Society

## Communications

### Cyanonaphthalene Diimide Semiconductors for Air-Stable, Flexible, and Optically Transparent n-Channel Field-Effect Transistors

Brooks A. Jones, Antonio Facchetti, Tobin J. Marks,\* and Michael R. Wasielewski\*

*Department of Chemistry, Materials Research Center, and the International Institute for Nanotechnology, Northwestern University, Evanston, Illinois 60208-3113*

*Received February 15, 2007*

Organic semiconductors offer potentially inexpensive active components in large-area and flexible optoelectronics such as complementary circuits (CMOS), light-emitting diodes (OLEDs), and photovoltaics (OPVs).<sup>1</sup> Because efficient charge transport in organic semiconductors is thought to proceed via hopping involving delocalized  $\pi$ -orbitals, such materials tend to be highly conjugated and thus excellent chromophores with optical extinction coefficients ( $\epsilon$ ) of  $\sim 10^4$  to  $\sim 10^6$  M<sup>-1</sup> cm<sup>-1</sup>. However, materials for transparent displays or charge-blocking layers in OLEDs/OPVs should ideally be transparent to visible light, requiring a  $>3$  eV band gap.<sup>2</sup> A common strategy for achieving wide band gap chromophores is to compress the molecular conjugation

length;<sup>3</sup> however, this frequently depresses charge-carrier mobility.<sup>4</sup> Consequently, attempts to fabricate transparent organic field-effect transistors (OFETs) with high mobility have generally yielded low band gap ( $<2.5$  eV) films with significant visible absorption.<sup>5</sup>

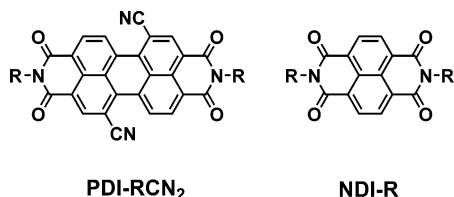
Recent studies of dicyanoperylene diimides (PDI-RCN<sub>2</sub>)<sup>6</sup> have demonstrated a unique combination of high electron mobility (as high as 0.6 cm<sup>2</sup> V<sup>-1</sup> s<sup>-1</sup>), environmental stability, and solution processability.<sup>6b</sup> Thus, PDI-RCN<sub>2</sub>s yield complementary organic logic and frequency-generating devices with unprecedented performance.<sup>6c-e</sup> However, the  $\sim 2.4$  eV PDI-RCN<sub>2</sub> band gap and  $\epsilon = 47000$  M<sup>-1</sup> cm<sup>-1</sup> renders 50 nm films intensely red to the eye and unsuitable for transparent organic optoelectronics.<sup>6a,6b</sup>

Previous research on core-unsubstituted naphthalene diimide (NDI) semiconductors demonstrated that this wide band gap ( $\sim 3$  eV) materials class can also exhibit high electron mobility, environmental stability, and solution

\* Corresponding authors. E-mail: t-marks@northwestern.edu (T.J.M.) and m-wasielewski@northwestern.edu (M.R.W.).

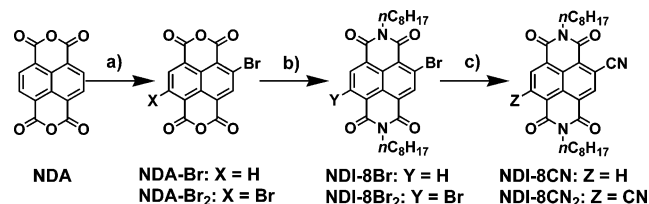
- (1) (a) *Printed Organic and Molecular Electronics*; Gamota, D. R., Brazis, P., Kalyanasundaram, K., Zhang, J., Eds.; Kluwer Academic Publishers: New York, 2004; p 695. (b) Malliaras, G.; Friend, R. *Phys. Today* **2005**, 58, 53–58. (c) Katz, H. E.; Bao, A. *J. Phys. Chem. B* **2000**, 104, 671–678.
- (2) (a) Wang, L.; Yoon, M.-H.; Lu, G.; Yang, Y.; Facchetti, A.; Marks, T. J. *Nat. Mater.* **2006**, 5, 893–900. (b) Artukovic, E.; Kaempgen, M.; Hecht, D.S.; Roth, S.; Gruner, G. *Nano Lett.* **2005**, 5, 757–760. (c) Hoffman, R. L.; Norris, B. J.; Wager, J. F. *Appl. Phys. Lett.* **2003**, 82, 733–735. (d) Masuda, S.; Kitamura, K.; Okumura, Y.; Miyatake, S.; Tabata, H.; Kawai, T. *J. Appl. Phys.* **2003**, 93, 1624–1630.

- (3) Turro, N. J. *Modern Molecular Photochemistry*; University Science Books: Sausalito, CA, 1991; p 628.
- (4) (a) Garnier, F.; Deloffre, F.; Horowitz, G.; Hajlaoui, R. *Synth. Met.* **1993**, 57, 4747–54. (b) Hutchison, G. R.; Ratner, M. A.; Marks, T. J. *J. Am. Chem. Soc.* **2005**, 127, 2339–2350.
- (5) See for example: (a) Ohta, H.; Kambayashi, T.; Nomura, K.; Hirano, M.; Ishikawa, K.; Takezoe, H.; Hosono, H. *Adv. Mater.* **2004**, 16, 312–316. (b) Choi, J.-M.; Hwang, D. K.; Kim, J. H.; Im, S. *Appl. Phys. Lett.* **2005**, 86, 123505.
- (6) (a) Ahrens, M. J.; Fuller, M. J.; Wasielewski, M. R. *Chem. Mater.* **2003**, 15, 2684–2686. (b) Jones, B. A.; Ahrens, M. J.; Yoon, M.-H.; Facchetti, A.; Marks, T. J.; Wasielewski, M. R. *Angew. Chem., Int. Ed.* **2004**, 43, 6363–6366. (c) Jung, T.; Yoo, B.; Wang, L.; Jones, B. A.; Facchetti, A.; Wasielewski, M. R.; Marks, T. J.; Dodabalapur, A. *Appl. Phys. Lett.* **2006**, 88, 183102. (d) Yoo, B.; Jung, T.; Basu, D.; Dodabalapur, A.; Jones, B. A.; Facchetti, A.; Wasielewski, M. R.; Marks, T. J., *Appl. Phys. Lett.* **2006**, 88, 082104. (e) Yoo, B.; Madgavkar, A.; Jones, B. A.; Nadkarni, S.; Facchetti, A.; Dimmler, D.; Wasielewski, M. R.; Marks, T. J.; Dodabalapur, A. *IEEE Electron Device Lett.* **2006**, 27, 737–739.



processability, but not in a single material.<sup>7</sup> NDI air stability typically requires the presence of fluorinated *N*-R groups, which also results in depressed mobility ( $0.06 \text{ cm}^2 \text{ V}^{-1} \text{ s}^{-1}$ ) relative to *N*-*n*-octyl NDI ( $0.16 \text{ cm}^2 \text{ V}^{-1} \text{ s}^{-1}$ ).<sup>7b</sup> In this communication, we report two new core-cyanated naphthalene diimide semiconductors, NDI-8CN and NDI-8CN<sub>2</sub> (Scheme 1),

**Scheme 1. Synthetic Route to NDI-8CN and NDI-8CN<sub>2</sub>, Where the Reaction Conditions Are: (a) Br<sub>2</sub>/I<sub>2</sub>, Oleum; (b) *n*-octyl Amine, HOAc; (c) CuCN, DMF.**



which represent the first air-stable, high-mobility, and transparent organic *n*-type semiconductors. Electrical properties are evaluated in bottom-gate (Si/SiO<sub>2</sub>) top-contact (Au) OFETs, along with thin film microstructure and morphology. Finally, the first visible region transparent OFET channel is fabricated. The syntheses of NDI-8CN and NDI-8CN<sub>2</sub> are achieved via a new NDI core bromination, cyanation sequence.

Typically, core-substituted NDIs are accessed via pyrene chlorination;<sup>8</sup> however, in the present work, NDA is brominated with I<sub>2</sub>/Br<sub>2</sub> to yield a mixture of monobrominated (NDA-Br) and dibrominated (NDA-Br<sub>2</sub>) products. Condensation with *n*-octyl amine is accomplished by refluxing in acetic acid, and the resulting mono- and dibromoisimides can be readily separated chromatographically. Interestingly, only a single substitutional isomer of NDI-8Br<sub>2</sub> is isolated, as evidenced by <sup>1</sup>H NMR and single-crystal X-ray diffraction (Figure 1), whereas perylene dianhydride dibromination yields a mixture of substitutional isomers.<sup>8d</sup> Previous rylene imide cyanations relied on Pd catalysts with Zn(CN)<sub>2</sub>,<sup>6a,6b</sup> however, cyanation of NDI-8Br and NDI-8Br<sub>2</sub> is accomplished with CuCN in DMF to afford NDI-8CN and NDI-8CN<sub>2</sub> in ~45% cyanation yield, without air-sensitive Pd catalysts.

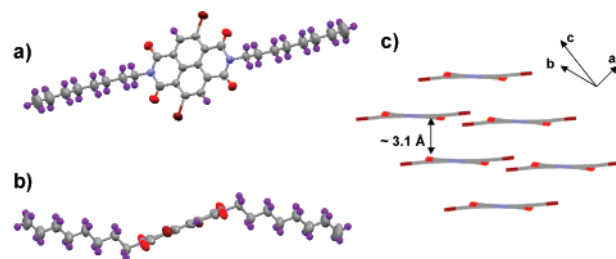


**Figure 1.** NDI-8Br<sub>2</sub> crystal structure depicting (a) the face-on view demonstrating the one substitutional isomer, (b) the side view depicting a nearly planar naphthalene core, and (c) the packing diagram demonstrating the small interplanar intermolecular distance of ~3.1 Å. *N,N'*-groups have been removed for clarity.

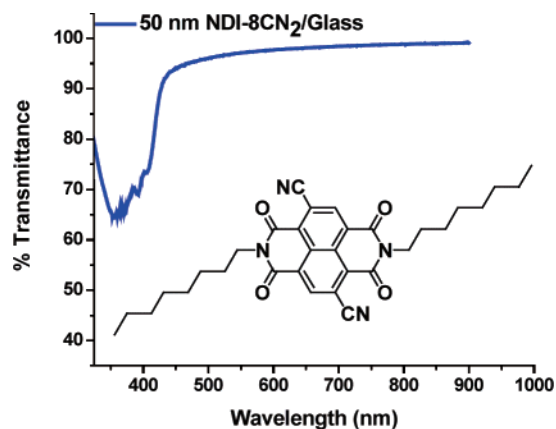


**Figure 2.** Transmission optical spectrum of a 50 nm vapor-deposited thin film of NDI-8CN<sub>2</sub> on glass demonstrating the impressive transparency of this material between 400 and 800 nm.

NDI-8CN and NDI-8CN<sub>2</sub> electronic structures were examined by cyclic voltammetry, optical spectroscopy, and photoluminescence. Electrochemical reduction potentials in dichloromethane vs S.C.E. are  $-0.22 \text{ V}$  for NDI-8CN and  $+0.08 \text{ V}$  for NDI-8CN<sub>2</sub>, consistent with systematic LUMO energy depression with increasing cyanation. Importantly, NDI-8CN<sub>2</sub> has a reduction potential similar to that of PDI-RCN<sub>2</sub> ( $-0.07 \text{ V}$  vs S.C.E.);<sup>6a-b</sup> therefore, the LUMO/charge-carrier energies in the NDI and PDI materials should be similar. Optical and photoluminescence spectroscopy of these NDI derivatives reveals a band gap of ~3 eV, reflecting the smaller conjugated core dimensions relative to PDIs.<sup>6a,6b</sup> Thus, thin films of these NDIs are transparent in the visible region (Figure 2).

Thin (50 nm) NDI-8CN and NDI-8CN<sub>2</sub> films were grown by physical vapor deposition ( $2 \times 10^{-6}$  Torr,  $0.2 \text{ Å/s}$ ) onto doped Si substrates having a 300 nm thermally grown SiO<sub>2</sub> dielectric. During film deposition, the growth temperature (*T<sub>d</sub>*) was varied to optimize the semiconductor film microstructure/morphology. All thin films were characterized by OFET measurements, X-ray diffraction (XRD), and tapping-mode AFM. Top-contact OFETs with  $100 \text{ μm}/5 \text{ mm}$  *S/D* width/length were fabricated by thermally depositing 50 nm thick gold electrodes onto the NDI films through a shadow mask.

OFET measurements performed in vacuum ( $\sim 10^{-6}$  Torr) reveal optimal average electron mobilities for NDI-8CN and NDI-8CN<sub>2</sub> films of  $4.7 \times 10^{-3} \text{ cm}^2 \text{ V}^{-1} \text{ s}^{-1}$  and  $0.15 \text{ cm}^2 \text{ V}^{-1} \text{ s}^{-1}$ , for *T<sub>d</sub>* values of 130 and 110 °C, respectively. These differences in mobility despite similar chemical structures

- (7) (a) Katz, H. E.; Johnson, J.; Lovinger, A. J.; Li, W. *J. Am. Chem. Soc.* **2000**, *122*, 7787–7792. (b) Katz, H. E.; Lovinger, A. J.; Johnson, J.; Kloc, C.; Seigrist, T.; Li, W.; Lin, Y.-Y.; Dodabalapur, A. *Nature* **2000**, *404*, 478–481. (c) Katz, H. E.; Otsuki, J.; Yamazaki, K.; Suka, A.; Takido, T.; Lovinger, A. J.; Raghavachari, K. *Chem. Lett.* **2003**, *32*, 508–509. (d) Katz, H. E.; Siegrist, T.; Schön, J. H.; Kloc, C.; Batlogg, B.; Lovinger, A. J.; Johnson, J. *ChemPhysChem* **2001**, *3*, 167–172.
- (8) (a) Thalacker, C.; Miura, A.; De Feyter, S.; De Schryver, F. C.; Würthner, F. *Org. Biomol. Chem.* **2005**, *3*, 414–422. (b) Würthner, F.; Ahmed, S.; Thalacker, C.; Debaerdemaeker, T. *Chem-Eur. J.* **2002**, *8*, 4742–4750. (c) Thalacker, C.; Röger, C.; Würthner, F. *J. Org. Chem.* **2006**, *71*, 8098–8105. (d) Würthner, F.; Stepanenko, V.; Chen, Z.; Saha-Moller, C. R.; Kocher, N.; Stalke, D. *J. Org. Chem.* **2004**, *69*, 7933–7939.

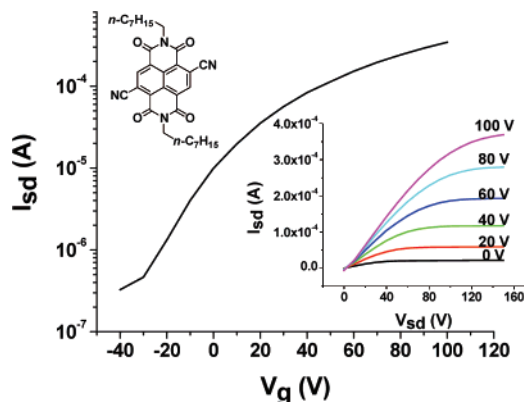


**Figure 3.**  $I$ – $V$  curves measured in air for NDI-8CN<sub>2</sub> films ( $T_d = 130$  °C) on Si/SiO<sub>2</sub> substrates after storage in ambient atmosphere for 5 months. The transfer plot yields an electron mobility of  $0.1 \text{ cm}^2 \text{ V}^{-1} \text{ s}^{-1}$  and  $I_{\text{on}}/I_{\text{off}} = 10^3$ . The inset of the output plot demonstrates the well-defined linear and saturation regime at the gate bias ( $V_g$ ) indicated above the trace.

are discussed with the AFM and XRD data below. Interestingly, OFET operation in ambient atmosphere reveals that the NDI-8CN devices undergo severe degradation of  $I$ – $V$  characteristics, whereas the NDI-8CN<sub>2</sub> devices exhibit stable operation with only a slightly lower maximum average mobility of  $0.11 \text{ cm}^2 \text{ V}^{-1} \text{ s}^{-1}$  (Figure 3). The NDI-8CN<sub>2</sub> robustness suggests that ambient stability can be extended to other rylene diimides via polycyanation to achieve reduction potentials  $\sim 0 \text{ V}$  vs S.C.E. The current on–off ratios ( $I_{\text{on}}/I_{\text{off}}$ ) can be as high as  $\sim 10^5$  for NDI-8CN and  $\sim 10^3$  for NDI-8CN<sub>2</sub> thin films. The lower  $I_{\text{on}}/I_{\text{off}}$  ratio of NDI-8CN<sub>2</sub> is due to high  $I_{\text{off}}$  ( $\sim 1 \times 10^{-6} \text{ A}$ ), which is likely due to dopants in the NDI-8CN<sub>2</sub> thin films or proximate dielectric layer.

AFM reveals similar polycrystalline morphologies for NDI-8CN and NDI-8CN<sub>2</sub> films, with ribbon-like grains until  $T_d \approx 90$  °C, and plate-like grains at higher  $T_d$  settings. XRD measurements on NDI-8CN and NDI-8CN<sub>2</sub> films indicate similar, highly textured microstructures, exhibiting only 00 $l$  reflections and with a  $d$ -spacing of  $18.2 \text{ \AA}$ . The primary difference in the film XRD data for the two materials is the presence of a second family of Bragg reflections in NDI-8CN<sub>2</sub> films grown at  $T_d > 90$  °C, corresponding to a  $d$ -spacing of  $20.2 \text{ \AA}$ . However, there is no obvious correlation between mobility and these additional reflections. Given the similar morphologies and microstructures of both NDI-8CN and NDI-8CN<sub>2</sub> films, the difference in mobility in vacuum is likely related to in-plane ordering, which cannot be rigorously evaluated with the present  $\theta/2\theta$  XRD and AFM data.

Top-contact bottom-gate transparent channel flexible n-type OFETs were fabricated with NDI-8CN<sub>2</sub> to demonstrate the unique materials properties. Thin NDI-8CN<sub>2</sub> films (50

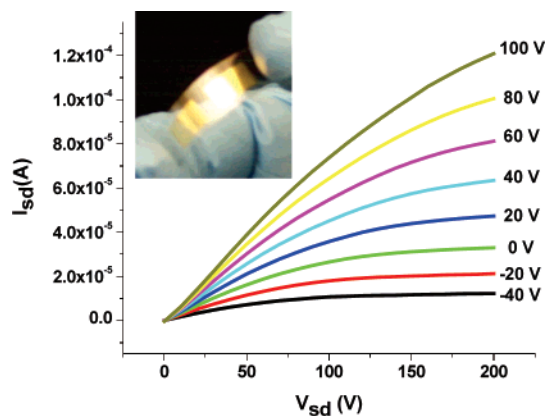


**Figure 4.** Output plot for a transparent, flexible OFET having a PEDOT:PSS gate, polymer gate dielectric, NDI-8CN<sub>2</sub> semiconductor, and Au source and drain, and exhibiting an electron mobility of  $0.03 \text{ cm}^2 \text{ V}^{-1} \text{ s}^{-1}$  in air. Inset: photograph of an array of  $\sim 100$  devices fabricated on overhead transparency film demonstrating transparency and flexibility.

nm) were vapor-deposited onto overhead transparency film coated with a spin-cast PEDOT:PSS polymeric gate and a P-UV-013 polymer dielectric.<sup>9</sup> Next, 20 nm gold source/drain electrodes were evaporated through a shadow mask onto the NDI-8CN<sub>2</sub> films to give an OFET of  $S/D$  width/length =  $100 \mu\text{m}/5 \text{ mm}$ . This air-stable, flexible, transparent OFET exhibits a mobility of  $0.03 \text{ cm}^2 \text{ V}^{-1} \text{ s}^{-1}$ ,  $V_{\text{th}} = -2 \text{ V}$ , and  $I_{\text{on}}/I_{\text{off}} \sim 10^3$  in ambient atmosphere (Figure 4). An analogous rigid device fabricated on an ultrasMOOTH ITO/glass substrate as a gate gives  $\mu = 0.08 \text{ cm}^2 \text{ V}^{-1} \text{ s}^{-1}$ ,  $V_{\text{th}} = 4 \text{ V}$ , and  $I_{\text{on}}/I_{\text{off}} \sim 10^3$  in ambient atmosphere.

In summary, new NDI core halogenation chemistry yields the first cyano NDIs. Dicyanation affords a similar reduction potential to PDI-RCN<sub>2</sub>s and imparts air-stability to the fluorine-free semiconductor. Utilizing PEDOT:PSS or ITO as the gate electrode and a polymer dielectric, the first high-mobility, air-stable, n-type transparent channel OFETs were fabricated with NDI-8CN<sub>2</sub>.

**Acknowledgment.** We thank ONR (N00014-05-1-0021) and AFOSR (STTR FA9550-05-0167) for funding and the Northwestern MRSEC (NSF DMR-0076097) for access to characterization facilities. We also thank Ms. Charlotte Stern for single-crystal X-ray data and Dr. He Yan of Polyera Corp. for transparent OFET substrates.

**Supporting Information Available:** Experimental details; spectral, electrochemical, film diffraction, AFM, electrical data, OFET fabrication details; CIF file. This material is available free of charge via the Internet at <http://pubs.acs.org>.

CM0704579

(9) Details of transparent device fabrication are contained in the Supporting Information.